l = 25 μm, r = 0.6 μm (measured from the cat rod outer segments encountered in our experiments), Q_{isom} = 0.67 [H. J. A. Dartnall, in *Handbook of Sensory Physiology, Photochemistry of Vision*, H. J. A. Dartnall, Ed. (Springer-Verlag, Berlin, 1972), vol. VII/1, pp. 122–145] and α = 0.016 μm^{-1} for light at 500 nm [P. A. Liebman, *ibid.*, pp. 481–528; F. I. Harosi, *J. Gen. Physiol.* **66**, 357 (1975)], A is calculated to be 0.35 μm^2. Since there are regional variations in the rod outer segment dimensions in the cat retina [R. H. Steinberg, M. Reid, P. L. Lacy, *J. Comp. Neurol.* **148**, 229 (1973)], this area should be considered to be only approximate.
16. R. Nelson, *J. Comp. Neurol.* **172**, 109 (1977).
17. N. W. Daw and A. L. Pearlman, *J. Physiol. (London)* **201**, 745 (1969); C. Enroth-Cugell, B. G. Hertz, P. Lennie, *ibid.* **269**, 273 (1977).
18. R. W. Rodieck and R. W. Ford, *Vision Res.* **9**, 1 (1969).
19. Many of the studies on rod adaptation in lower vertebrates were made with intracellular recordings. In these studies, the observed Weber-Fechner behavior of rod desensitization [see, for example, (*3*)] extends over a broader range of background intensities than measured with the suction-pipette method (*5*). This difference suggests that voltage-sensitive conductances at the rod inner segment, which shape the voltage response of the cell to light, may contribute to background adaptation by extending the Weber-Fechner range.
20. K. Nakatani, T. Tamura, K.-W. Yau, manuscripts in preparation.
21. Penn and Hagins suggested that simple response compression according to the Michaelis relation (given by the form $\hat{r} = I/(I + \sigma)$, where $\hat{r}$ is normalized response amplitude, I is light intensity, and σ is a constant) could directly lead to the Weber-Fechner type of desensitization. This is unlikely, however, because this relation should predict a flash sensitivity that decreases as the square of background intensity (which can be seen by differentiating the above relation with respect to I), rather than as the first power of I as in the Weber-Fechner relation. See also E. H. Adelson, *Vision Res.* **22**, 1299 (1982).
22. R. H. Steinberg, *J. Physiol. (London)* **217**, 93 (1971).
23. ———, M. Reid, P. L. Lacy, *J. Comp. Neurol.* **148**, 229 (1973).
24. P. Sterling, *Annu. Rev. Neurosci.* **6**, 149 (1983); ———, M. A. Freed, R. G. Smith, *J. Neurosci.* **8**, 623 (1988).
25. H. B. Barlow and W. R. Levick, *J. Physiol. (London)* **196**, 2P (1968); P. Hammond and C. R. James, *ibid.* **216**, 99 (1971); R. W. Rodieck and W. A. H. Rushton, *ibid.* **254**, 759 (1976).
26. H. B. Barlow, W. R. Levick, M. Yoon, *Vision Res. Suppl.* **3**, 87 (1971).
27. J. E. Dowling, *The Retina: An Approachable Part of the Brain* (Belknap-Harvard, Cambridge, 1987).
28. We thank M. L. Hudak and M. B. Sachs for kindly providing us with the cats at the end of their experiments, N. W. Daw for discussion, and L. W. Haynes and B. Minke for comments on the manuscript. Supported by a grant from the U.S. National Eye Institute. K.-W. Y. is an investigator of the Howard Hughes Medical Institute.

29 March 1989; accepted 12 June 1989

Limbic Seizures Increase Neuronal Production of Messenger RNA for Nerve Growth Factor

CHRISTINE M. GALL* AND PAUL J. ISACKSON

Nerve growth factor (NGF) produced by telencephalic neurons provides critical trophic support for cholinergic neurons of the basal forebrain. In situ hybridization and nuclease protection analyses demonstrate that limbic seizures dramatically increase the amount of messenger RNA for NGF in the neurons of the hippocampal dentate gyrus within 1 hour of seizure onset and in broadly distributed neocortical and olfactory forebrain neurons some hours later. The increased messenger RNA species is indistinguishable from messenger RNA for transcript B of the β subunit of NGF from mouse submandibular gland. Thus, the expression of a known growth factor is affected by unusual physiological activity, suggesting one route through which trophic interactions between neurons in adult brain can be modified.

NERVE GROWTH FACTOR, WHICH promotes the growth and maintenance of sympathetic and sensory neurons of the peripheral nervous system (*1*), is differentially expressed in the mammalian brain with the highest levels of NGF mRNA present in hippocampus (*2*). NGF synthesized by forebrain neurons may provide critical trophic support for cholinergic neurons of the basal forebrain, and disturbances in this relation may be involved in age-related neuropathologies such as Alzheimer's disease (*3, 4*). In support of this idea, it has been demonstrated that NGF is retrogradely transported from hippocampus to cholinergic neurons in septum and basal forebrain (*5*), and that infusion of NGF can prevent the degeneration of these same cholinergic cells after transection of their connections with hippocampus (*6*). Here we report that limbic seizures cause a rapid and pronounced increase in the expression of mRNA for NGF in the granule cells of the rat hippocampus. Moreover, a delayed increase was found in cortical areas, suggesting that the spread of seizure activity triggers changes in the expression of NGF mRNA throughout much of the forebrain.

Adult (280 to 350 g) male Sprague-Dawley rats (Simonsen Labs) were used. Recurrent limbic seizures were induced by the placement of a unilateral electrolytic lesion in the dentate gyrus hilus (*7*). Such lesions produce bilateral epileptiform electroencephalogram (EEG) activity in the hippocampus and behavioral seizures of the limbic kindling type (*8*) without causing secondary neuronal degeneration in the contralateral hippocampus. Hippocampal paroxysmal discharges begin 1.5 to 2 hours after the lesion and recur intermittently for 8 to 10 hours. Paired control rats received either ketamine-xylazine anesthesia alone or were anesthetized with sodium pentobarbital (50 mg/kg), and a lesion was placed in the dentate gyrus hilus with an insulated platinum-iridium wire. Such platinum wire lesions do not produce hippocampal EEG or behavioral seizures (*9*).

For in situ hybridization, experimental animals with behaviorally verified seizures and paired control rats were killed 2.5 (n = 1), 3 (n = 9), 4 (n = 3), 5 (n = 2), 6 to 7 (n = 5), 10 (n = 2), 17 (n = 3), and 24 (n = 5) hours after surgery by overdose with sodium pentobarbital and intracardial perfusion with 4% paraformaldehyde in 0.1M phosphate buffer (pH 7.4) (*10*). In the greater number of these studies, ^{35}S-labeled RNA probes complementary to the coding regions for either mature mouse (*11, 12*) (Fig. 1A) or rat β-NGF (*13*) were used. We have obtained qualitatively identical results with a 550-base RNA probe prepared from the 5′ end of a guinea pig β-NGF cDNA clone (*14*). Although similar seizure-induced changes in hybridization to NGF mRNA were observed bilaterally, the description here will be limited to regions contralateral to lesion placement. Controls for the specificity of hybridization included treatment of tissue sections with ribonuclease A before normal hybridization and hybridization of sections with labeled "sense" RNA sequences (*15*). No cellular labeling was observed in tissue from experimental or anesthetic-control rats processed under either control condition.

In untreated rats, in situ hybridization to NGF mRNA is greatest in the hippocampal formation. In tissue autoradiograms, subpopulations of neurons within the dentate gyrus hilus (Fig. 2A) and scattered within and around stratum pyramidale of hippocampus proper and subiculum were moderately densely labeled with the ^{35}S-labeled cRNA probe. As could be seen most clearly in tissue processed with the rat β-NGF cRNA sequence, stratum granulosum was also labeled, but with lower densities of autoradiographic grains. This distribution is essentially in agreement with other reports (*13, 16*), although we observed greater differences in the densities of hybridization to

C. M. Gall, Department of Anatomy and Neurobiology, University of California, Irvine, CA 92717.
P. J. Isackson, Department of Anatomy and Neurobiology, and Department of Biological Chemistry, University of California, Irvine, CA 92717.

*To whom correspondence should be addressed.

different neuronal populations than had been indicated by others. Glial cells in hippocampal neuropil or the surrounding white matter were not labeled. Outside hippocampus, scattered neurons within the basal forebrain, rostral piriform cortex, and portions of the amygdaloid complex were moderately densely labeled, whereas occasional neurons within superficial layers of more caudal olfactory cortex were labeled with lower autoradiographic grain densities.

A large increase in hybridization was evident within stratum granulosum of experimental animals killed from 2.5 to 6 hours after the hilus lesion (HL) (Fig. 2). Calibrated densitometric measures of film autoradiograms indicate that in these HL rats, hybridization within stratum granulosum was 20- to 28-fold more dense than in paired controls [for example, in one experiment, in which the rat β-NGF cRNA probe was used, densitometric estimates of hybridization within stratum granulosum were 33 ± 14 (SD) and 953 ± 199 cpm per 25 μg of protein in a control and 3-hour HL rat, respectively]. The full depth of the granule cell layer was densely labeled in tissue autoradiograms, giving the impression that all, or at least the great majority, of dentate gyrus granule cells contained high quantities of NGF mRNA at these times. In addition, hybridization was increased slightly within superficial layers of entorhinal cortex, but appeared normal in both hippocampal stratum pyramidale and neocortex.

By 17 to 24 hours after the HL, hybridization to NGF mRNA within stratum granulosum had declined, but was still 2- to 12-fold higher than in control rats. However, at these survival intervals hybridization of the cRNA probe was increased slightly within stratum pyramidale and was dramatically elevated in entorhinal cortex, piriform cortex, posterocorticomedial amygdala, and layers II, III, and VI of broad fields of neocortex (Fig. 2). The magnitude of the HL-induced increase in hybridization within neocortex was greatest in rats that exhibited greater numbers of strong behavioral seizures; in one such rat, killed 24 hours after the HL, hybridization within layers II and III of lateral neocortex was approximately 30-fold more dense than in the paired control rat (266 ± 52 versus 9 ± 2 cpm per 25 μg of protein, respectively).

The increase in NGF mRNA observed with in situ hybridization was confirmed by nuclease protection assay of RNA purified from the combined hippocampal CA1 and dentate gyrus subfields and the entorhinal cortex with two probes derived from nonoverlapping segments of a mouse submandibular gland cDNA clone (Fig. 1). Experiments with a ^{32}P-labeled RNA probe from the same region of the mouse NGF cDNA used for in situ hybridization (that is, complementary to mature mouse β-NGF sequence) demonstrated a greater than sixfold increase in NGF mRNA in the dentate gyrus–CA1 samples from rats 3 hours after HL as compared to anesthetic-control rats (Figs. 1, A and C). As for the in situ hybridization results, no increase in NGF mRNA was seen in tissue from lesion-control rats (in which a nonseizure-producing lesion was placed with platinum-iridium wire). Thus, the HL-induced increase in hybridization is dependent on seizure activity, as opposed to the direct damage or deafferentation produced by the lesion.

A single-stranded DNA probe derived from the 5′ end of a mouse submandibular gland cDNA for β-NGF transcript A (*11*) was used for S1 nuclease protection assay to further confirm the specificity of the in situ hybridization results and to characterize the 5′ end of NGF transcripts induced by seizures (Fig. 1, B and D). Two predominant NGF transcripts and other less abundant transcripts differing at the 5′ end are present in the mouse submandibular gland (*17, 18*). NGF transcript A of the mouse encodes a protein precursor of 307 amino acids, whereas transcript B lacks the 127-bp second exon and encodes a smaller precursor containing 241 amino acids. A shorter fragment of the probe is protected by RNA from the dentate gyrus and entorhinal cortex of HL rats than is protected by RNA from mouse submandibular gland or guinea pig prostate gland (which predominantly contain NGF transcript A) (Fig. 2D). The same RNA protection pattern can be seen in samples of these brain regions from anesthetic control rats after longer film exposures. These data suggest that the NGF

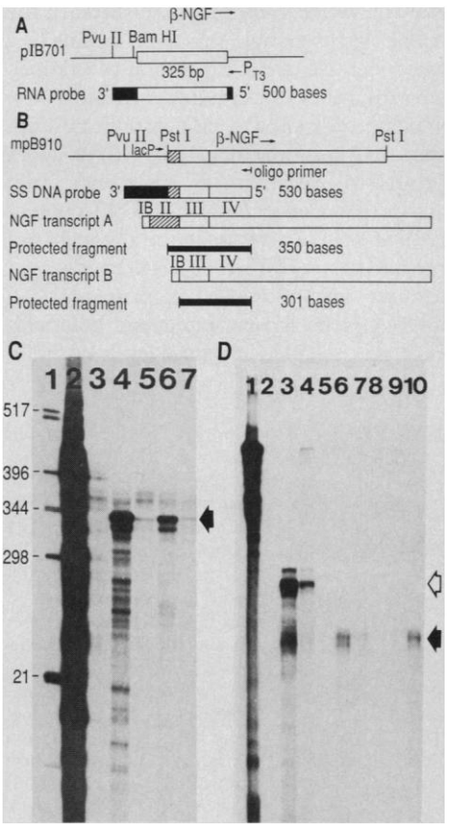

Fig. 1. S1 nuclease protection assay of NGF mRNA induced in rats by seizure activity (*29, 30*). (**A**) The 500-base ^{32}P-labeled RNA probe, used for the analysis in (C), that was transcribed with T3 RNA polymerase from Pvu II–digested pIB701 [pIB701 is a plasmid construction containing a 325-bp fragment of the mouse submandibular gland NGF cDNA (*11, 14*), which encodes amino acids 6 to 112 of the mature NGF]. The RNA probe shown contains 145 bases of vector sequence at its 3′ end and 30 bases at its 5′ end (designated by filled boxes). (**B**) The 530-base ^{32}P-labeled DNA probe used for the protection assay in (D) was prepared from an mp18 template containing a 900-bp Pst I fragment of a partial mouse submandibular gland cDNA (*11*). A 15-base oligonucleotide complementary to bases 445 to 460 of the full-length NGF transcript A (*11*) was used as a primer for synthesis of the probe from the single-stranded M13 template with the Klenow fragment of *Escherichia coli* DNA polymerase I in the presence of [α-^{32}P]dATP, followed by Pvu II digestion and polyacrylamide gel purification of the single-stranded DNA probe. The probe contains 200 bases of mp18 vector sequence (filled box), 49 bases from exon 2 (which is present in mouse NGF transcript A, but not in transcript B), the 124-base exon 3 and 177 bases of exon 4. NGF transcript A is predicted to protect 350 bases of probe 1, whereas transcript B will protect 301 bases. (**C**) Electrophoretic analysis of S1 nuclease protection of the RNA probe in (A). Lane 1: Hinf I–digested pBR322 fragments end-labeled with ^{32}P; lane 2: wheat germ transfer RNA alone, no nuclease digestion; lane 3: wheat germ transfer RNA alone; lane 4: 0.1 μg of male mouse submandibular gland polyadenylated RNA; lane 5: 10 μg of total RNA from the dentate gyrus of anesthetic-control rats; lane 6: dentate gyrus 3 hours after HL; lane 7: dentate gyrus of platinum-lesion–control rats. RNA from the dentate gyrus 3 hours after HL (lane 6) protects a fragment identical in size to that of the submandibular gland RNA (lane 4) and contains greater than sixfold more NGF mRNA (arrow) than controls (lanes 5 and 7). (**D**) Electrophoretic analysis of S1 nuclease protection of probe in (C). Lane 1: wheat germ transfer RNA alone, no nuclease digestion; lane 2: wheat germ transfer RNA alone; lane 3: 0.1 μg of male mouse submandibular gland polyadenylated RNA; lane 4: 1 μg of guinea pig prostate polyadenylated RNA; lane 5: 10 μg of total RNA from the dentate gyrus of anesthetic-control rats; lane 6: dentate gyrus 3 hours after HL; lane 7: dentate gyrus 24 hours after HL: lane 8: 10 μg of total RNA from the entorhinal cortex of anesthetic control rats; lane 9: entorhinal cortex 3 hours after HL; and lane 10: entorhinal cortex 24 hours after HL. The open arrow indicates the 350-base fragment protected by transcript A, and the filled arrow indicates the 301-base fragment protected by transcript B. Only the smaller fragment is protected by RNA from the brain tissue with the greatest quantities evident in the dentate gyrus 3 hours after HL (lane 6) and entorhinal cortex at 24 hours after HL (lane 10).

mRNA induced by seizure corresponds to transcript B, which predominates in mouse and rat brain (*17, 18*), although it may also include transcripts differing from both A and B in the region 5′ to exon 3.

Our in situ hybridization and nuclease protection analyses indicate that HL-induced seizures stimulate a rapid increase in NGF mRNA, which appears first in the dentate gyrus granule cells and later in olfactory and neocortical sites. The finding that NGF mRNA expression in the adult brain can be readily and massively increased is unexpected. Although a 50% increase in hippocampal NGF mRNA occurs after deafferentation in the neonatal rat (*19*), neither hippocampal deafferentation in the adult (*20*) nor sensory deprivation during development (*18*) alters NGF mRNA content of forebrain neurons, suggesting that the expression of mRNA for this growth factor in brain is not dependent on physiological activity. However, our results establish that such a link does in fact exist, but do not determine which aspects of the intense activity produced by seizures are responsible for it. Two possibilities merit consideration. First, increased expression of NGF mRNA may occur in brief surges triggered by intense neuronal activity associated with particular physiological or behavioral states, with mRNA levels falling quickly back to baseline values. Possibly relevant to this, the seizure-induced elevation of NGF mRNA in dentate gyrus declined from 1.5 to 15 hours after seizure onset, even though recurrent seizure activity continued through much of this interval. Second, increased NGF expression may depend on some aberrant physiological feature of seizures and thus be an aspect of pathophysiology. Studies with brief periods of high-frequency stimulation that do not elicit seizures should be of value in distinguishing between these possibilities.

In addition to establishing a connection between physiological activity and NGF expression, our experiments allow the analysis of the processing and transport of NGF protein in the brain (*21*). Moreover, the production of increased levels of a biologically active form of NGF in response to seizure would suggest the possibility of increasing endogenous levels of NGF by physiological stimulation for therapeutic purposes.

The consequences of increased expression of NGF mRNA are perhaps best viewed as part of the constellation of genomic changes that follow recurrent limbic seizures. In the dentate gyrus granule cells these include (i) a rapid increase in the expression of immediate-early genes (for example, *c-fos* and *c-jun*), which encode known and putative transcription activating factors (*22*); (ii) a more protracted elevation of preproenkephalin and preproneuropeptide Y mRNA content (*23*); and (iii) a decrease in the abundance of preprodynorphin mRNA (*24*). In this context the seizure-induced increase in NGF mRNA is both very rapid and transient. Like *c-fos* mRNA, maximal levels of NGF mRNA in the granule cells are reached less than 6 hours after the HL, at which time preproenkephalin mRNA is on the rise and preproneuropeptide Y mRNA is not yet increased.

It is possible that the brief increase in NGF expression sets in motion a longer lasting cascade of genomic events in the hippocampus and basal forebrain with *c-fos* or other immediate-early gene responses acting as intermediaries. NGF receptor mRNA is present within hippocampus (*25*), and NGF stimulates the production of mRNA from c-*fos* (*26*) and neuropeptide genes (*27*) in cultured cells. In addition, limbic seizures, shown here to stimulate NGF expression, also promote elaboration of axonal branches and somatic spines (*28*) on the dentate gyrus granule cells. It is not implausible then that the rapid seizure-stimulation of increased levels of NGF mRNA, and the presumed increase in the production of the trophic factor itself, represent critical steps in structural and genomic responses of the hippocampal neurons to intense physiological activity. Moreover, there is evidence that the biosynthetic activities and structural integrity of cholinergic neurons that project to the hippocampus are dependent on NGF (*6*). Therefore, the effects of electrical activity on NGF described here suggest one means by which physiological activity could maintain and modify the chemical characteristics of this component of limbic circuitry.

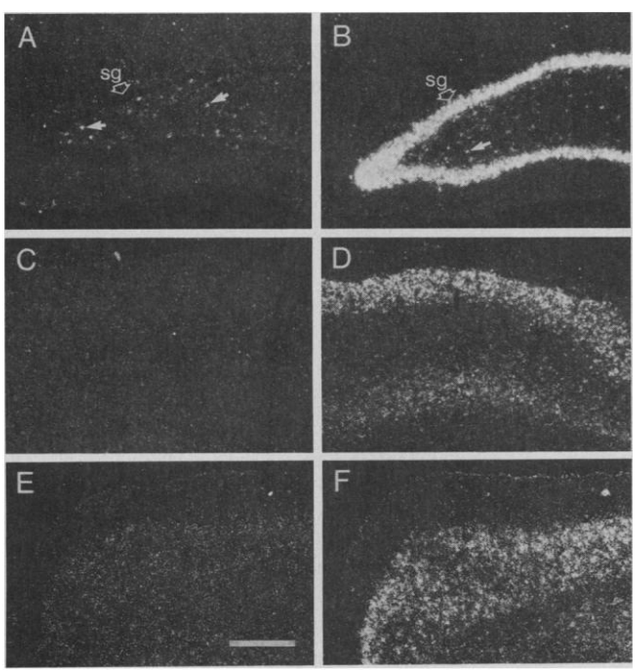

Fig. 2. Photomicrographs showing the autoradiographic localization of in situ hybridization of ^{35}S-labeled mouse β-NGF cRNA within sections through hippocampal dentate gyrus (**A** and **B**), lateral neocortex (**C** and **D**), and piriform cortex (**E** and **F**) of an anesthetic-control rat (A, C, and E) and paired experimental-seizure rats (B, D, and F) that were killed 4 hours (B) and 17 hours (D and F) after a contralateral HL. There is an increased density of autoradiographic grains (seen here as white under dark-field illumination) overlying stratum granulosum (sg) of the 4-hour HL rat (B) relative to the paired control (A). (Arrowheads indicate labeled neurons within the dentate gyrus hilus in each case.) In lateral neocortex (C and D), seizure-induced increases in hybridization are evident in both superficial (top white lamina) and deep layers with neurons in intermediate lamina remaining unlabeled. In (C) to (F), the cortical surface appears at the top of each micrograph; there is an absence of labeled cells in the adjacent cortical layer I, which is enriched in glial cell bodies. Bar, 390 μm for (A) and (B); 500 μm for (C) to (F).

REFERENCES AND NOTES

1. H. Thoenen and Y. A. Barde, *Physiol. Rev.* **60**, 1285 (1980).
2. A. Korshing *et al.*, *EMBO J.* **4**, 1389 (1985); D. L. Shelton and L. Reichardt, *Proc. Natl. Acad. Sci. U.S.A.* **83**, 2714 (1986); S. R. Whittemore *et al.*, *ibid.*, p. 817.
3. S. H. Appel, *Ann. Neurol.* **10**, 499 (1981).
4. F. Hefti, *ibid.* **13**, 109 (1983); F. Hefti and W. J. Weiner, *Neurology* **20**, 275 (1986).
5. M. E. Schwab *et al.*, *Brain Res.* **168**, 473 (1979).
6. F. Hefti, *J. Neurosci.* **6**, 2155 (1986); L. F. Kromer, *Science* **235**, 214 (1987).
7. Animals were anesthetized with either ketamine (50 mg/kg) and xylazine (10 mg/kg) or ether, and a small electrolytic lesion was stereotaxically placed in the dorsal dentate gyrus hilus with an insulated stainless steel wire and anodal current of 0.8 mA for 7 s.
8. R. Racine, *Clin. Neurophysiol.* **32**, 281 (1972); M. Baudry, G. Lynch, C. Gall, *J. Neurosci.* **6**, 3430 (1986); C. M. Gall, R. Pico, J. C. Lauterborn, *Peptides* **9**, 79 (1988).
9. K. A. Campbell, B. Bank, N. W. Milgram, *Exp. Neurol.* **86**, 506 (1984); C. M. Gall and P. J. Isackson, unpublished observations.
10. Free-floating, 20-μm thick tissue sections were transferred sequentially through 0.1*M* glycine in 0.1*M* phosphate buffer (*p*H 7.2) (PB), proteinase K (1 μg/ml), and 50 m*M* EDTA in 0.1*M* tris (*p*H 8) (30 min at 37°C) and 2× saline sodium citrate (SSC) (30 min) (*p*H 7); incubated in hybridization solution [50% formamide, 10% dextran sulfate, 0.7% Ficoll, 0.7% polyvinyl pyrrolidone, bovine serum albumin (350 mg/ml), yeast transfer RNA (0.15 mg/ml), denatured herring sperm DNA (0.33 mg/ml), and 20 μ*M* dithiothreitol] for 1 hour at 60°C; and then incubated in fresh hybridization solution containing the cRNA probe at a density of 1×10^6 cpm/100 μl and 40 μ*M* dithiothreitol for

16 to 20 hours at 60°C. Sections were then washed through 4× SSC, treated with ribonuclease A (20 μg/ml) in 10 m*M* tris-saline (*p*H 8) with 1 m*M* EDTA for 30 min at 45°C, washed through descending concentrations of SSC to 0.1× SSC at 60°C for 1 hour, mounted onto gelatin-coated slides, and air-dried. The distribution of hybridization was evaluated with both film (Amersham βmax) and emulsion (Kodak NTB2) autoradiographic techniques with exposure times of 3 to 5 days and 2 to 6 weeks, respectively. For densitometric analysis, film autoradiograms were calibrated relative to ^{35}S-labeled brain paste standards (exposed, with tissue, to each sheet of film) by using The Microcomputer Imaging Device (Imaging Research).

11. J. Scott *et al.*, *Nature* **302**, 538 (1983).
12. Antisense mouse NGF RNA probes (370 bases) were transcribed from Bam HI linearized pIB701 (Fig. 2A) with T3 RNA polymerase in the presence of [^{35}S]uridine 5′-(α-thio)triphosphate.
13. S. R. Whittemore *et al.*, *J. Neurosci. Res.* **20**, 403 (1988).
14. M. A. Schwarz *et al.*, *J. Neurochem.* **52**, 1203 (1989).
15. Control sense strand RNA probes (380 bases) for mouse NGF were transcribed from Hind III linearized pIB701 (Fig. 2A) with T7 RNA polymerase.
16. C. Ayer-LeLievre *et al.*, *Science* **240**, 1339 (1988); P. D. Rennert and G. Heinrich, *Biochem. Biophys. Res. Commun.* **138**, 813 (1986).
17. R. H. Edwards *et al.*, *Nature* **319**, 784 (1986).
18. M. J. Selby, R. Edwards, F. Sharp, W. J. Rutter, *Mol. Cell. Biol.* 7, 3057 (1987).
19. S. R. Whittemore *et al.*, *J. Neurosci.* 7, 244 (1987).
20. L. Larkfors, I. Stromberg, T. Ebendal, L. Olson, *J. Neurosci. Res.* **18**, 525 (1987).
21. R. H. Edwards, M. J. Selby, P. D. Garcia, W. J. Rutter, *J. Biol. Chem.* **263**, 6810 (1988).
22. J. I. Morgan, D. R. Cohen, J. L. Hempstead, T. Curran, *Science* **237**, 192 (1987); D. W. Saffen *et al.*, *Proc. Natl. Acad. Sci. U.S.A.* **85**, 7795 (1988); J. D. White and C. M. Gall, *Mol. Brain Res.* **3**, 21 (1987).
23. C. Gall, *J. Neurosci.* **8**, 1852 (1988); J. D. White, C. M. Gall, J. F. McKelvy, *ibid.* 7, 753 (1987); C. M. Gall and J. D. White, in *The Hippocampus, New Vistas*, V. Chan-Palay, Ed. (Liss, New York, in press); G. L. Yont, C. M. Gall, J. D. White, *Soc. Neurosci. Abstr.*, in press.
24. B. J. Morris *et al.*, *Neurosci. Lett.* **80**, 298 (1987); B. J. Morris *et al.*, *Proc. Natl. Acad. Sci. U.S.A.* **85**, 3226 (1988).
25. C. R. Buck, H. J. Martinez, M. V. Chao, I. B. Black, *Dev. Brain Res.* **44**, 259 (1988).
26. M. E. Greenberg *et al.*, *Science* **234**, 80 (1986); J. I. Morgan and T. Curran, *Nature* **322**, 552 (1986).
27. J. M. Allen *et al.*, *Brain Res.* **427**, 1 (1987).
28. T. Sutula, X. X. He, J. Cavazos, G. Scott, *Science* **239**, 1147 (1988); M. Bundman *et al.*, *Soc. Neurosci. Abstr.* **14**, 833 (1988).
29. Total RNA was purified by the method of Chirgwin *et al.* (*30*) from pooled CA1–dentate gyrus and retrohippocampal cortex (including entorhinal cortex) samples from control and HL rats. RNA samples (usually 10 μg of total RNA) with 25 μg of wheat germ transfer RNA were annealed to an excess of ^{32}P-labeled DNA or RNA probe for 16 hours at 57°C in 80% formamide, 0.4*M* NaCl, 40 m*M* Pipes (*p*H 6.4), and 1 m*M* EDTA in a total volume of 10 μl. Samples were diluted to 200 μl with 0.25*M* NaCl, denatured salmon sperm DNA (200 μg/ml), 1 m*M* $ZnSO_4$, and 30 m*M* sodium acetate (*p*H 4.6) and digested with 200 units of S1 nuclease (Pharmacia) for 2 hours at 37°C. Ethanol-precipitated samples were separated by electrophoresis on 6% polyacrylamide:7*M* urea gels and exposed to Kodak XAR5 film 1 to 5 days.
30. J. M. Chirgwin *et al.*, *Biochemistry* **24**, 5294 (1979).
31. We thank J. Scott for providing the mouse β-NGF cDNA clone; S. Whittemore for providing the rat β-NGF cDNA clone; G. Lynch and R. Bradshaw for helpful comments; and J. Lauterborn, K. Murray, and D. Benson for technical assistance. Supported by NS26748 and NS00915 to C.M.G. and NS24747 and a grant from Alzheimer's Disease and Related Disorders Association to P.J.I.

14 February 1989; accepted 29 June 1989

Neuronal Correlates of Subjective Visual Perception

NIKOS K. LOGOTHETIS AND JEFFREY D. SCHALL*

Neuronal activity in the superior temporal sulcus of monkeys, a cortical region that plays an important role in analyzing visual motion, was related to the subjective perception of movement during a visual task. Single neurons were recorded while monkeys (*Macaca mulatta*) discriminated the direction of motion of stimuli that could be seen moving in either of two directions during binocular rivalry. The activity of many neurons was dictated by the retinal stimulus. Other neurons, however, reflected the monkeys' reported perception of motion direction, indicating that these neurons in the superior temporal sulcus may mediate the perceptual experience of a moving object.

NEURONS IN THE VISUAL CORTEX of higher mammals respond only to specific properties of visual stimuli (*1*). One way to distinguish neuronal activity related to perceptual processes rather than to physical stimulus characteristics is to expose the visual system to stimuli that allow more than one percept. When the visual cues provided are enough to dictate one description of the visual scene, perception is unique and stable. But when the sensory data are insufficient for just one interpretation, rival possibilities are entertained and perception becomes ambiguous, switching between the alternatives. Binocular rivalry, a percept that ensues when dissimilar stimuli are presented to the two eyes, is a typical instance of perceptual instability (*2*). Because such stimuli cannot be fused by the cyclopean visual system, the perception alternates between the stimulus seen by the right eye alone or the left eye alone. For example, when the right eye is presented with upward movement and the left eye with downward movement, the perceived motion alternates between up and down.

The middle temporal (MT) and medial superior temporal areas in the superior temporal sulcus (STS) contain neurons that analyze visual motion (*3*), but it is not known whether such activity can be directly related to the conscious perception of movement. To investigate this possibility, we used rhesus monkeys because they experience binocular rivalry (*4*).

Three rhesus monkeys were trained in a motion discrimination task. Two vertically drifting horizontal gratings were generated on a video monitor and presented independently to the two eyes through a stereoscopic viewer. Eye movements were monitored with a scleral search coil, and a disparity calibration was performed to position the

Department of Brain and Cognitive Sciences, Massachusetts Institute of Technology, Cambridge, MA 02139.

*Present address: Department of Psychology, Vanderbilt University, Nashville, TN 37240.

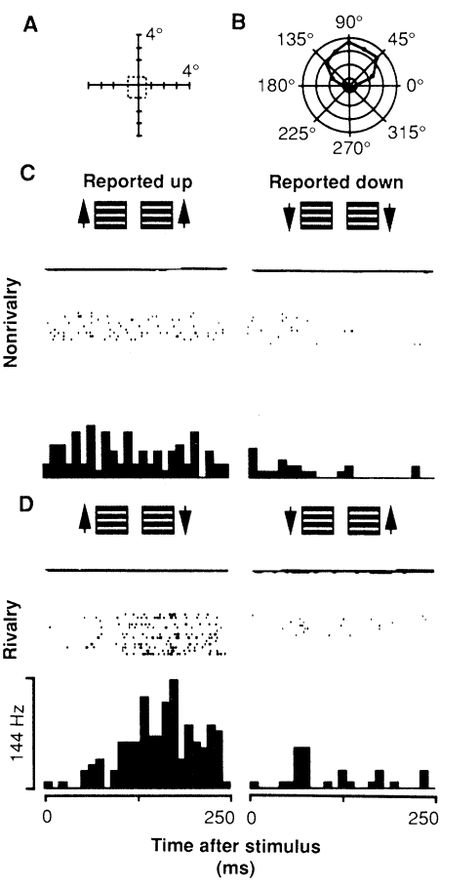

Fig. 1. Response of single unit in the STS to nonrivalrous and rivalrous stimuli. (**A**) Receptive field position. This cell had a small central receptive field. (**B**) Direction tuning curve. Each point represents the average discharge rate in response to drifting gratings. Each concentric circle represents 30 spikes per second. The cell preferred upward motion. (**C** and **D**) Responses during nonrivalrous (C) and rivalrous (D) grating presentation when the monkey reported seeing up (left) and down (right). The gratings depict the type of motion presented to each eye. Beneath the gratings, the vertical eye movement traces are superimposed for each trial. Single unit activity is illustrated by rasters and time histograms of the average firing rate. The eye position traces, rasters, and histograms are aligned on the onset of the nonrivalrous or rivalrous grating presentations.